Surface Science Letters

Inter- and intraband inelastic scattering of hot surface state electrons at the Ag(1 1 1) surface

L. Vitali [a,*], P. Wahl [a], M.A. Schneider [a], K. Kern [a], V.M. Silkin [b,c], E.V. Chulkov [b,c], P.M. Echenique [b,c]

[a] *Max-Planck-Institut für Festkörperforschung, Heisenbergstr.1, D-70569 Stuttgart, Germany*
[b] *Materrielen Fisika Saila, Kimika Fakultatea, Euskal Herriko, Unibertsitatea, 1072 Posta kutxatila, 20018 Donostia, Basque Country, Spain*
[c] *Donostia International Physics Center (DIPC), 1072 Posta kutxatila, 20018 Donostia, Basque Country, Spain*

Abstract

The phase coherence length and the corresponding lifetime of hot electrons in the surface state band of Ag(1 1 1) have been measured with a low temperature STM for energies from the Fermi level to 3 eV. A divergence of the lifetime from a $(E - E_F)^{-2}$ behavior has been observed for energies lower than 400 meV. Theoretical analysis in terms of electron–electron and electron–phonon scattering mechanisms shows that the energy dependence of the lifetime is accounted for by the competition between intra- and interband electron–electron inelastic scattering and electron–phonon contributions.
© 2002 Elsevier Science B.V. All rights reserved.

Keywords: Silver; Scanning tunneling microscopy; Electron–solid interactions, scattering, diffraction

Surface state electrons can control a large variety of physical processes as adsorption, electron screening and in general electron dynamics and transport [1,2]. The knowledge of the phase coherence length L_Φ, i.e. the length which surface state electrons can travel without losing their phase coherence, is thus of fundamental importance. While the elastic mean free path of electrons is not affected by electron–electron scattering, because such a process does not lead to any loss in the total momentum, the phase coherence length is very sensitive to phase randomizing electron–electron and electron–phonon collisions. The measurement of L_Φ, or equivalently of the lifetime of the quasiparticle $\tau_\Phi = L_\Phi m^* / \hbar k_\parallel$, provides a direct information on the electron–electron and electron–phonon interaction, where m^* is the reduced mass and $k_\parallel$ the wave vector of the surface state electrons.

On metal surfaces the electron lifetimes have been determined using different techniques as photoemission [1,3], time-resolved two photon-photoemission [4–7], and scanning tunneling

* Corresponding author. Tel.: +49-7116891538; fax: +49-7116891662.
E-mail address: l.vitali@fkf.mpg.de (L. Vitali).

microscopy (STM) [8,9]. While the first two integrate over a macroscopic area and therefore can be affected by the presence of surface defects or impurities that reduce the lifetime, STM enables to select perfect terraces for the lifetime determination. For the Ag(1 1 1) surface local scanning tunneling spectroscopy (STS) and dI/dV mapping on clean terraces [8,9] as well as inside confined regions, e.g. islands [10] or artificial quantum resonators [11,12], has been used to determine the lifetime of the surface state electrons. However, the local density of states (LDOS) inside the confinements is modified with respect to the LDOS observed on clean terraces. It is therefore not clear if in the latter experiments the reported lifetime is only due to the surface state electrons and is not affected by e.g. the adsorbate species delimiting the confined region in the case of artificial quantum resonators.

The lifetimes of low energy surface state electrons on Ag(1 1 1) reported in this letter have been determined from direct measurement of the phase coherence length. The approach is based on the quantitative analysis of the amplitude decay of the quantum mechanical interference pattern at step edges [9]. The interference patterns ("standing waves") die away within a short distance of the step because electrons eventually scatter from one quantum state into another, destroying the phase coherence. Thus the lifetime during which the electron remains in a specific quantum state before scattering is directly reflected in the distance over which the waves persist away from the step edge. The experiments are the first momentum resolved lifetime measurements of the pristine surface spanning the entire energy interval from the Fermi level to the band edge. By comparison with theoretical calculations we are able to identify the relevant relaxation mechanism in terms of intra- and interband inelastic electron–electron scattering and electron–phonon coupling.

In the experiment, large defect-free terraces with a very low impurity concentration have been prepared cleaning the Ag(1 1 1) by Ar-sputtering and annealing cycles. The experiments were performed at 6 K with a home built UHV STM [13] using a tungsten tip. The dI/dV images have been acquired by a lock-in technique superimposing a
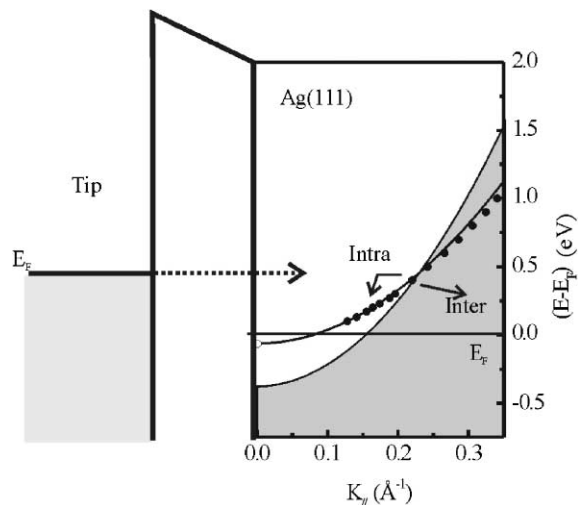

Fig. 1. Scheme of the tunneling process of hot electrons in the surface state band. Dots indicate the $k_\parallel$ for Energies below 1 eV at which the lifetime of the electron has been experimentally evaluated. These can relax through intra- or interband scattering.

sinusoidal signal with amplitude ΔV to the applied sample bias. Particular attention has been paid in selecting surface areas free of impurities and other potential scatterers for a distance larger than the mean free path of the electrons. This assures that the coherence length of the electrons is not influenced by other static scattering centers. STM allows in a very flexible way to inject electrons in a metal at chosen energies above the Fermi level. The schematic principle of the tunneling process is shown in Fig. 1. An electron tunnels from the Fermi level of the tip into an unoccupied level of the metal from where after a short time it will decay to the ground state. In this figure the surface state dispersion relation ($m^* = 0.4m_e$ and $E_\Gamma = -65$ meV [1,14]) is plotted together with the projected bulk band ($m^* = 0.25m_e$ and $E_\Gamma = -380$ meV [15,16]). Circular dots in Fig. 1 indicate the energy below 1 eV where the lifetime of the hot electrons has been experimentally evaluated.

Fig. 2a shows a dI/dV map (which is proportional to the LDOS) of the surface on the upper terrace in proximity of step (bright line marked with an arrow). An averaged series of line scans parallel to the dashed line in the dI/dV map
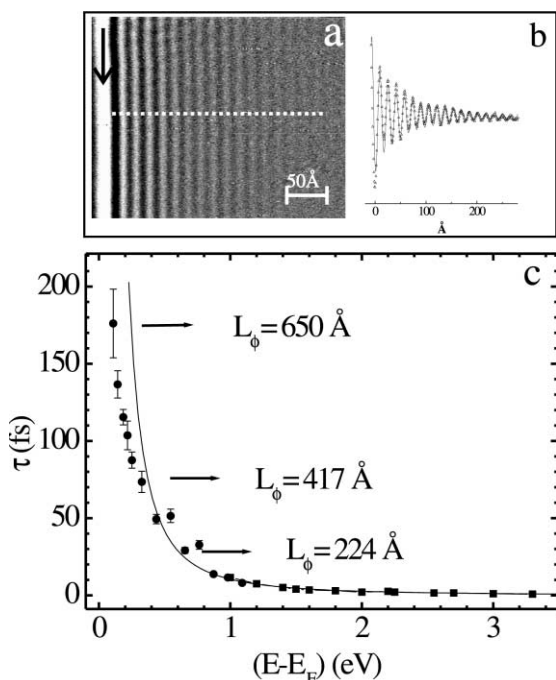
Fig. 2. Experimental lifetime of hot surface state electrons at the Ag(1 1 1) surface. (a) dI/dV map of the Ag(1 1 1) surface in proximity of a step edge (marked with an arrow). Image size $\sim 320 \times 250$ Å^2, achieved at 330 mV, with 31 mV lock-in modulation (peak-to-peak). (b) Amplitude decay on the upper terrace perpendicular to the step edge obtained by averaging over several line scans of the dI/dV map in a), from which the decay length L_Φ is determined to be 417 Å. (c) Measured lifetime as a function of energy; Solid symbols are the newly acquired low energy data (circles) and the data of our earlier measurement (solid squares) taken from [9]. The solid line is a fit of the data from [9] (i.e. at high energies) to the $(E - E_F)^{-2}$ behavior of a free electron gas in the Fermi liquid model with a prefactor of 10.4 fs eV^2 [9].

showing an oscillatory behavior whose periodicity is bias dependent, is presented in Fig. 2b. Surface state electrons elastically scattered by a repulsive potential localized at the step edge [25] return at the tip position where they superimpose coherently with the incoming electron. This creates an oscillatory pattern in the LDOS due to interference. Inelastic scattering processes that destroy the phase coherence of an electron traveling between tip and step lead to a decreasing amplitude of the oscillation as a function of the distance from the step. This decay of the LDOS pattern reflects therefore

the phase coherence at the clean surface, which is free of defects. At a given energy E, the LDOS at the step can be described by [9]

$$\rho_{\text{step}}(E, x) \propto \left(1 - r(k_\parallel) e^{-2x/L_\Phi} J_0(2k_\parallel x)\right) \tag{1}$$

where J_0 is the Bessel function of zeroth order and r is the reflection amplitude.

The exponential factor in Eq. (1) accounts for the finite coherence length L_Φ of the electrons, which is determined by inelastic scattering processes outside the range of the scattering potential of the step. The amplitude of the quantum interference pattern decays with increasing distance x from the step as a consequence of phase randomizing events such as the inelastic electron–electron and electron–phonon scattering processes on the clean terrace, which correspondingly reduce the lifetime $\tau(E)$. Eq. (1) was used in the region $x > 1.5\pi k_\parallel$ from the step position, which is well outside the region where the step potential itself modifies the LDOS. A fitting procedure, which accounts for the applied lock-in modulation and for the broadening of the Fermi–Dirac distribution at $T = 6$ K, has been performed in order to obtain the wave vector parallel to the surface $k_\parallel(E)$ and the phase coherence length of the electrons L_Φ at each given energy. It was then checked that the defect-free terrace width at which the measurement was taken was at least twice the obtained L_Φ. The result of this analysis is shown in Fig. 2c for the full energy range 0.1–3 eV including our earlier data from Ref. [9]. The experimental data are found to scale with $(E - E_F)^{-2}$ above 0.5 eV but substantially deviate from the quadratic scaling at lower energies.

For completeness the lifetime of holes at the $\overline{\Gamma}$-point of the surface state band has also been evaluated. Measurements of the differential conductance vs. sample-voltage V have been performed with a lock-in technique in open feedback loop conditions at single points on a wide defect-free terrace. At the onset of the surface state the LDOS shows a sharp rise from which the lifetime of the holes can be extrapolated [8]. With a refined analysis we took carefully into account the effect of the lock-in modulation and temperature and obtained an average line width of 5.5 meV,

corresponding to a lifetime of 120 fs for the holes at this energy. [1] The line width is consistent although somewhat smaller than what has been experimentally observed with photoemission [1] and with previous STM studies [8,17].

Our theoretical calculation of the electron–electron contribution to the inverse lifetime, Γ, is based on the GW approximation for the quasiparticle self-energy [18]. Since fully first-principles three dimensional calculations of surface quasiparticle dynamics for metals with d-electrons are computationally not yet feasible [24] we use a model in which charge density and one-electron potential varies only in z-direction perpendicular to the surface and is constant in the (x, y)-plane [21]. In this model the inverse lifetime of a quasiparticle with energy E_0 and momentum $k_\parallel$ is written in terms of the 2D Fourier transforms of the self-energy

$$\Gamma = -2 \int \int \phi_0^*(z) \text{Im} \Sigma(z, z'; k_\parallel, E_0) \phi_0(z') \, \mathrm{d}z \, \mathrm{d}z' \tag{2}$$

where the $\text{Im}\Sigma$ is

$$\begin{aligned} &\text{Im} \Sigma(z, z'; k_\parallel, E_0) \\ &= \frac{1}{(2\pi)^2} \sum_{E_n}^{E_F < E_n < E_0} \phi_n^*(z') \phi_n(z) \\ &\quad \times \int \text{Im} W \left(z, z'; k_\parallel - q_\parallel, E_0 - E_n \right. \\ &\quad \left. + \frac{k_\parallel^2}{2m_0^2} - \frac{q_\parallel^2}{2m_n^2} \right) \mathrm{d}q_\parallel. \end{aligned} \tag{3}$$

---

[1] To extract the line width of holes from the onset of the surface states the derivative of the $\mathrm{d}I/\mathrm{d}V$ curve has been calculated. This transforms the surface states onset into a peak centered at the E_0-point. The peak has been fitted with a Voigt function in which the FWHM of the Lorentzian and of the gaussian components account for the line width and the lock-in modulation contribution respectively. The Lorentzian contribution has been obtained as fitting parameter while the corresponding gaussian width has been fixed as the applied lock-in modulation. This fitting procedure allows to measure the lifetime from the onset of the surface state avoiding possible geometrical uncertainties in the location of the surface state onset which are intrinsic in the method proposed by Li et al. [8].

Here $\text{Im} W(z, z'; k_\parallel, E_0 - E_f)$ is the two-dimensional Fourier transform of the imaginary part of the screened Coulomb interaction, $E_0(\phi_0(z))$ and $E_n(\phi_n(z))$ are the energies (wave functions) of the initial and final states, respectively, describing electron motion perpendicular to the surface, and m_0 and m_n are corresponding effective masses. The energies E_n and wave functions $\phi_n(z)$ have been evaluated by using a well-tested model potential of Ref. [19].

This approach has been successfully applied to the calculation of quasiparticle lifetimes in the wide gap s–p surface state band and image potential states at the center of the Brillouin zone for the (1 1 1) surfaces of noble metals and Be(0 0 0 1) [17,20,21]. In contrast to the surface state band bottom which is well separated from bulk states [15,19] the surface state band approaches the bulk band edge for energies above E_F and enters bulk continuum at ~ 0.46 eV losing its surface weight. This behavior is of crucial importance to understand the physics of the electron decay in the surface state. To take this fact into account we modify the wave function of the surface state at $k_\parallel \neq 0$ for $E > E_F$ by recalculating $\phi(z)$ for the relevant energy gap width and the surface state energy in the same way as it was done for the surface band bottom [19,21]. The evaluation of Γ with the recalculated momentum dependent surface state wave functions leads to the significant reduction (by factor of 4 at $E = 0.5$ eV) of intraband contribution and to much better agreement with the measured results. Another potentially important point is the role of d-states in the quasiparticle decay. The potential [19] correctly describes the s–p valence states just below E_F and for $E > E_F$ which are included in inter- and intraband transitions in Eq. (3). d-states do not directly participate in these transitions because they are located rather deep in energy, nevertheless they can influence the electron decay through screening. Due to the small momentum transfer involved and to the fact that the surface state electrons are separated from the d-orbitals the screening effect due to d-electrons is rather small [22], and does not influence seriously the decay rate of electrons in the surface state. Besides the electron–electron part Γ_{e-e} of the decay we have also performed the calculation of the

electron–phonon contribution Γ_{e-ph} [23] that in-
cludes both the bulk and surface phonon modes.
For energies which are higher than the Debye
temperature of Ag and which are of interest to the
present work this contribution has a constant va-
lue of 3.6 meV.

To compare the theoretical results with the ex-
perimental data we estimated the effect of a single
step on Γ_{e-e}. Assuming that the electron self-
energy is the same both for an ideal surface and for
a surface with a step (this is the case for distances
relatively far from the step) one obtains that the
effect of the step is scaled as $1/R$, where R is the
terrace width. For terraces used in the present
experiments the step contributes 0.1% of the ideal
surface Γ_{e-e}. Neglecting this contribution in Fig. 3
we compare the measured and calculated results
in terms of an inverse lifetime $\Gamma = \hbar/\tau$ scaled by
$1/(E - E_F)^2$ for energies from 0.1 to 1 eV (for
energies $E > 0.8$ eV our theoretical method is less
valid because of approximations used). In the
$1/(E - E_F)^2$ units the conventional Fermi liquid
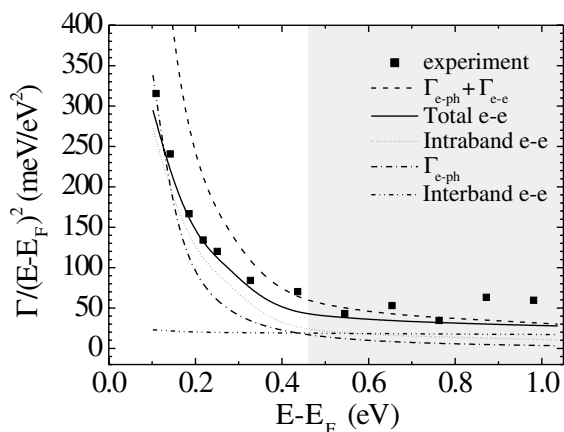theory gives $\Gamma =$ constant as a function of energy

Fig. 3. Comparison between the experimental inverse lifetime Γ
(solid symbols) and the calculated Γ (lines) plotted as $\Gamma/(E -
E_F)^2$ vs. $(E - E_F)$. The various inelastic channels contributing to
the calculated $\Gamma_{e-e} + \Gamma_{e-ph}$ (dashed line) are given in different
line formats (see legend in the figure). The deviation from the
quadratic behavior found at high energies in Fig. 2 is due to
contributions from intraband (2D) electron–electron scattering
(dotted) and electron–phonon interaction Γ_{e-ph} (dash-dotted).
The gray shaded area of the plot marks the region where the
surface state overlaps in energy with the projected bulk bands.

and any deviation of scaled inverse lifetime will
show non-free electron gas behavior of the lifetime
broadening. The comparison of experiment and
theory allows to analyze the most important con-
tributions to the decay rate in different energy in-
tervals. In the figure the experimental data are
shown as solid squares whereas the theoretical
calculation is shown as lines. The calculated line
widths Γ due to inter- (3D) and intraband (2D)
electron–electron Γ_{e-e} scattering, the electron–
phonon interaction Γ_{e-ph}, and the line width due to
all the inelastic scattering processes $\Gamma_{tot} = \Gamma_{e-e} +
\Gamma_{e-ph}$ are shown separately. We see that for ener-
gies in excess of 0.35 eV the theoretical calculation
of Γ_{tot} agrees well with the measured data. For
$E > 0.5$ eV the interband contribution from bulk
states becomes the largest one, however it still re-
mains comparable with the intraband contribu-
tion. For high energies electron–phonon scattering
becomes negligible at low temperatures. For en-
ergies lower than 0.35 eV we find that the mea-
sured lifetimes are larger (i.e. Γ is smaller) than the
lifetimes predicted but in reasonable agreement.
The intraband transitions and Γ_{e-ph} scattering are
competitive processes at energy lower than 400
meV and are responsible for the deviation from the
quadratic behavior. For these energies the surface
state shows less bulk like behavior than for higher
energies. The increase of the contribution from
intraband transitions is attributed to a stronger 2D
character of the transitions screened by the un-
derlying 3D electron system [17] and enhanced by
$\ln((E - E_F)/E_F)$ [26]. Therefore the experimental
data show the transition between different domi-
nant scattering mechanisms when the electron en-
ergy approaches the Fermi level.

In conclusion, low temperature STM measure-
ments of the lifetimes have been carried out for hot
electrons in the surface state band of Ag(1 1 1) for
energies $0.1 < E < 3$ eV. The results are compared
to calculations that permit to identify the rela-
tive strength of inelastic scattering mechanisms.
Whereas for energies above 1 eV scattering with
bulk electrons dominates over electron–electron
scattering in the surface state band, this latter
mechanism becomes the dominating inelastic elec-
tron–electron interaction for energies below 0.4
eV. It has been shown that for this energy range

inelastic intraband electron–electron scattering and electron–phonon interactions control the deviation of the inverse lifetime from the quadratic behavior observed at higher energies.

Acknowledgements

References

[1] N. Memmel, Surf. Sci. Rep. 32 (1998) 91.

[2] S. Datta, Electronic Transport in Mesoscopic Systems, Cambridge University Press, Cambridge, 1995.

[3] F. Reinert, G. Nicolay, S. Schmidt, D. Ehm, S. Hüfner, Phys. Rev. B 63 (2001) 115415.

[4] J.D. McNeil, R.L. Lingle Jr., N.H. Ge, C.M. Wong, R.E. Jordan, C.B. Harris, Phys. Rev. Lett. 79 (1997) 4645.

[5] U. Höfer, I.L. Shumay, Ch. Reuss, U. Thomann, W. Wallauer, Th. Fauster, Science 277 (1997) 1480.

[6] I.L. Shumay, U. Höfer, Ch. Reuss, U. Thomann, W. Wallauer, Th. Fauster, Phys. Rev. B 58 (1998) 13974.

[7] E. Knoesel, A. Hotzel, M. Wolf, J. Electron. Spectrosc. Relat. Phenom. 88 (1998) 577.

[8] J. Li, W.-D. Schneider, R. Berndt, O.R. Bryant, S. Crampin, Phys. Rev. Lett. 81 (1998) 4464.

[9] L. Bürgi, O. Jeandupeux, H. Brune, K. Kern, Phys. Rev. Lett. 82 (1999) 4516.

[10] J. Li, W.-D. Schneider, R. Berndt, S. Crampin, Phys. Rev. Lett. 80 (1998) 3332.

[11] J. Kliewer, R. Berndt, S. Crampin, New J. Phys. 3 (2001) 22.1.

[12] K.-F. Braun, K.-H. Rieder, Phys. Rev. Lett. 88 (2002) 096801.

[13] O. Jeandupeux, L. Bürgi, A. Hirstein, H. Brune, K. Kern, Phys. Rev. B 59 (1999) 15926.

[14] L. Bürgi, L. Petersen, H. Brune, K. Kern, Surf. Sci. 447 (2000) L157.

[15] R. Panagio, R. Matzdorf, G. Meister, A. Goldmann, Surf. Sci. 336 (1995) 113.

[16] S.D. Kevan, R.H. Gaylord, Phys. Rev. B 36 (1987) 5809.

[17] J. Kliewer, R. Berndt, E.V. Chulkov, V.M. Silkin, P.M. Echenique, S. Crampin, Science 288 (2000) 1399.

[18] P.M. Echenique, J.M. Pitarke, E.V. Chulkov, A. Rubio, Chem. Phys. 251 (2000) 1.

[19] E.V. Chulkov, V.M. Silkin, P.M. Echenique, Surf. Sci. 391 (1997) L1217, 437 (1999) 330.

[20] P.M. Echenique, J. Osma, M. Machado, V.M. Silkin, E.V. Chulkov, J.M. Pitarke, Progr. Surf. Sci. 67 (2001) 271.

[21] E.V. Chulkov, V.M. Silkin, M. Machado, Surf. Sci. 482–485 (2001) 693.

[22] A. García-Lekue, J.M. Pitarke, E.V. Chulkov, A. Liebsch, P.M. Echenique, Phys. Rev. Lett. 89 (2002) 096401.

[23] A. Eiguren, B. Hellsing, F. Reinert, G. Nicolay, E.V. Chulkov, V.M. Silkin, S. Hüfner, P.M. Echenique, Phys. Rev. Lett. 88 (2002) 066805.

[24] C. López-Bastidas, J.A. Maytorena, A. Liebsch, Phys. Rev. B 65 (2002) 035417.

[25] M.F. Crommie, C.P. Lutz, D.M. Eigler, Nature 363 (1993) 524.

[26] G.F. Giuliani, J.J. Quinn, Phys. Rev. B 26 (1982) 4421.